Symmetry-Resolved Vibrational Spectroscopy for the C $1s^{-1}2\pi_u$ Renner-Teller Pair States in CO$_2$

H. Yoshida,[1] K. Nobusada,[2] K. Okada,[3] S. Tanimoto,[3] N. Saito,[4] A. De Fanis,[5] and K. Ueda[5,*]

[1]*Department of Physical Science, Hiroshima University, Higashi-Hiroshima 739-8526, Japan*
[2]*Division of Chemistry, Graduate School of Science, Hokkaido University, Sapporo, 060-0810, Japan*
[3]*Department of Chemistry, Hiroshima University, Higashi-Hiroshima 739-8526, Japan*
[4]*National Institute of Advanced Industrial Science and Technology, Tsukuba 305-8568, Japan*
[5]*Institute of Multidisciplinary Research for Advanced Materials, Tohoku University, Sendai 980-8577, Japan*

Symmetry-resolved excitation spectra have been measured for the Renner-Teller pair states A_1 and B_1 split from the core-excited C $1s^{-1}2\pi_u$ state in CO$_2$. A vibrational progression with the spacings of $\sim$145 meV is found in both the A_1 and B_1 spectra at different energies and assigned to the symmetric stretching mode caused in the B_1 linear state, with the help of *ab initio* calculations. Appearance of the vibrations in the A_1 spectrum is interpreted as due to nonadiabatic coupling between the A_1 and B_1 states via the bending motion.

Remarkable progress has been achieved in the development of the synchrotron radiation sources and the soft x-ray monochromators in the past decade. Nowadays one can record the excitation spectrum of free molecules in the vicinity of the K edges of the light elements with the photon bandwidth narrower than the natural lifetime width of the core-excited state and thus see the detailed structures which reflect the molecular vibrations in the core-excited state [1–3].

The angle-resolved ion yield spectroscopy provides information about the symmetry of inner-shell excited states of linear molecules which cannot be obtained by the conventional absorption spectroscopy [4–7]. This method relies on the fact that the core-hole decay and fragmentation occur much faster than the molecular rotation and thus the direction of the ion ejection relative to the electric vector E of the linearly polarized light reflects the direction of the dipole moment relative to the molecular axis, i.e., the axial recoil approximation is valid [8,9]. The angle-resolved ion yield spectroscopy with a high-resolution monochromator on the linearly polarized soft x-ray beam line has proved to be a powerful tool for unambiguous assignments of the Rydberg states of linear molecules (see, for example, [10,11] and references therein). The symmetry resolution, however, has been considered to be lost, when symmetry lowering, such as linear to bent, takes place in the core-excited state [11,12].

In this Letter, we demonstrate that the symmetry-resolved excitation spectra arising from the transitions to the symmetry-lowered core-excited states can also be obtained. Here we discuss the C $1s \rightarrow 2\pi_u$ resonance as a specific example. In the case of the C $1s$ excitation to the lowest unoccupied molecular orbital $2\pi_u$, the dipole transition moment is perpendicular to the molecular axis. The C $1s^{-1}2\pi_u$ core-excited state splits into Renner-Teller pair states, referred to as the static Renner-Teller effect

[12–15]. The lower-energy state becomes bent while the upper one remains linear. The bent state has an electron in the π orbital that lies in the bending plane of the molecule (in-plane A_1 in C_{2v}) while the linear state has an electron in the π orbital that lies perpendicular to the bending plane (out-of-plane B_1 in C_{2v}). In this Letter, we probe these two states separately and present the vibrationally resolved A_1 and B_1 excitation spectra.

The idea of the experiment is as follows. We employ the well-established experimental approach, the angle-resolved energetic-ion yield spectroscopy. Figure 1 illustrates the concept of the experiment. We detect fragment ions in the directions parallel (0°) and perpendicular (90°) to the E vector of the incident light. The C $1s \rightarrow 2\pi_u$ excitation takes place preferentially for the molecule whose axis is aligned in the direction perpendicular to the E vector. The fragment ions from the linear CO$_2$ molecule are detected only by the detector at 90° [12]. As a result, the detection of the fragment ions by the detector at 0° directly reflects the bending motion of the molecule. Here the key point is that the bending motion is in the directions parallel to the dipole moment for the A_1 state and perpendicular to the dipole moment for the B_1 state. The planes in which the bending motion proceeds are illustrated in Fig. 1. The molecules and the planes of the bending motion can be rotated around the E vector in the figure without loss of generality. Thus it is clear that the ions originating from the B_1 excitation cannot be detected at 0°, as long as the axial recoil approximation [8,9] is valid.

We introduce here the quantities $I(0)$ and $I(90)$ for ion yields recorded by the 0° and 90° detectors, respectively, and $I(A_1)$ and $I(B_1)$ for ion yields originating from the A_1 and B_1 excitations, respectively. These quantities are normalized in such a way to satisfy the following relation:
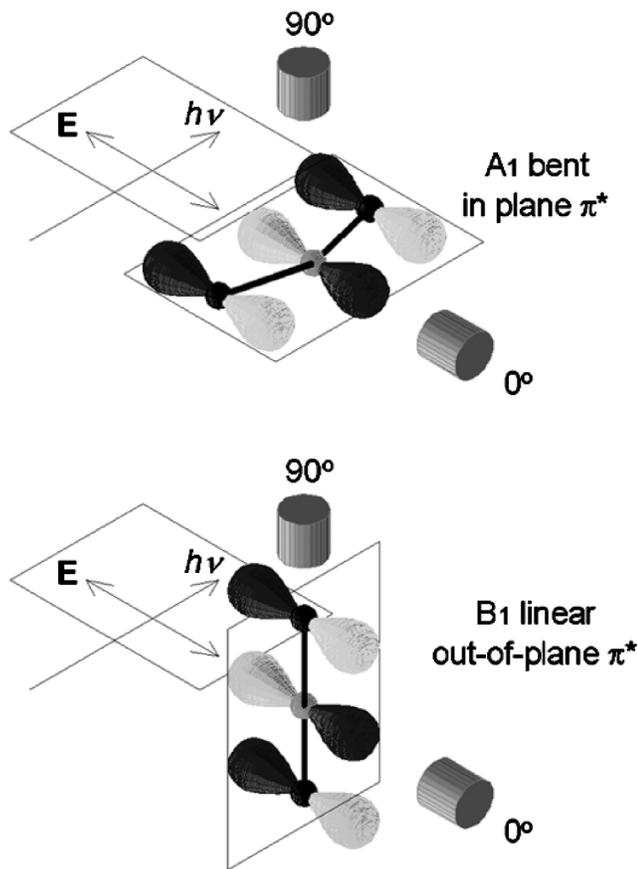
FIG. 1. A schematic view of the geometry of the $2\pi_u$ orbitals in the C $1s^{-1}2\pi_u$ states.

$$I(A_1) + I(B_1) = I(0) + 2I(90). \tag{1}$$

Because $I(0)$ does not include the contribution from the B_1 excitation we can express $I(0) = \alpha I(A_1)$ with α being a branching ratio of $I(A_1)$ to $I(0)$. We then have

$$I(A_1) = \frac{I(0)}{\alpha}, \qquad I(B_1) = 2I(90) - \frac{1-\alpha}{\alpha}I(0). \tag{2}$$

Thus we can extract $I(A_1)$ and $I(B_1)$ from $I(0)$ and $I(90)$ if we know the values of α. The value of α can be related to the ratio $p \equiv I(B_1)/I(A_1)$:

$$\alpha = \frac{I(0)}{I(0) + 2I(90)}(1 + p). \tag{3}$$

The values of p have been measured at several photon energies across the C $1s \rightarrow 2\pi_u$ resonance by means of the triple-ion-coincidence momentum-imaging technique [16]. Thus we can extract $I(A_1)$ and $I(B_1)$ from the measurements of $I(0)$ and $I(90)$.

The experiment was carried out on the c branch of the soft x-ray photochemistry beam line BL27SU at SPring-8 [17]. The light source is a figure-8 undulator and provides linearly polarized light: the E vector is horizontal for the first-order harmonic light and vertical for the 0.5th order harmonic light [18]. The experimental setup and procedure were described elsewhere [19]. Briefly, the

two energetic-ion yield curves were obtained by using two energetic-ion ($KE > 6$ eV) detectors mounted at 0° and 90° with respect to the E vector. Total ion yield (TIY) was measured simultaneously with a different detector. The photon energy scale was calibrated by use of C $1s$ to $3p$ and $4p$ Rydberg transitions [20]. The photon energy resolution was estimated to be ~30 meV by analyzing absorption and photoelectron spectra of several samples.

Figures 2(a) and 2(b) show the TIY and the angle-resolved energetic-ion yield spectra of CO_2 measured across the C $1s \rightarrow 2\pi_u$ resonance. In the spectra, the baseline, which includes contributions from the valence ionization and the ionziation by the second-order light, was removed. A similar TIY spectrum was measured by Kukk *et al.* [15] with a resolution similar to the one adopted here. They observed a vibrational progression with spacing of 151 meV and assigned it to the symmetric stretching mode (ν_1) of the linear B_1 state. Similar angle-resolved ion yield spectra for the C $1s \rightarrow 2\pi_u$ resonance were observed also by Adachi *et al.* [12] with lower resolution. They ascribed the shift of the peak positions, for the energetic-ion yield spectra recorded in
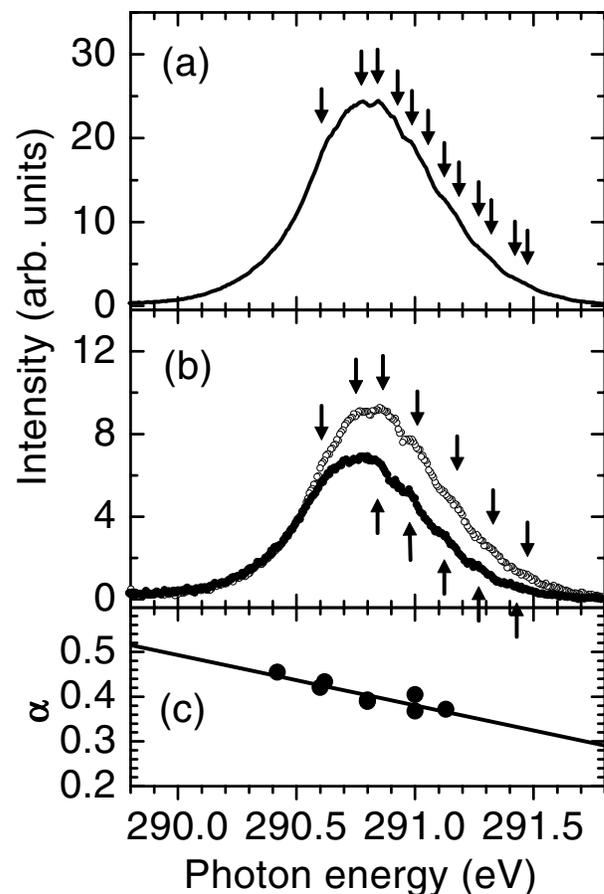
FIG. 2. (a) TIY and (b) angle-resolved energetic-ion yield spectra of CO_2 measured across the C $1s \rightarrow 2\pi_u$ resonance. In (b), the solid and open circles are recorded at 0° and 90°, respectively. The arrows indicate the positions where one can see the structures by eye. (c) Photon energy dependence of the α factor (see text).

the directions parallel and perpendicular to the E vector, to the Renner-Teller splitting, but they did not resolve any vibrational structures.

In the TIY spectrum in Fig. 2(a), we notice more complex structure than that discussed by Kukk *et al.* [15]: we can recognize at least two vibrational progressions with vibrational spacing of $\sim$145 meV. Similar vibrational structures can also be seen in angle-resolved spectra $I(0)$ and $I(90)$ in Fig. 2(b). We obtained the values of α from the values of p [16] and the measured spectra $I(0)$ and $I(90)$, using Eq. (3), and plotted the results in Fig. 2(c). The values of α exhibit weak energy dependence. We thus carried out a linear fitting to the data points. Finally we have extracted symmetry-resolved excitation spectra $I(A_1)$ and $I(B_1)$ from α, $I(0)$, and $I(90)$.

Figures 3(a) and 3(c) show the symmetry-resolved excitation spectra $I(A_1)$ and $I(B_1)$, respectively. Only one vibrational progression appears in the $I(B_1)$ spectrum. We can recognize one vibrational progression also on the high-energy side of the $I(A_1)$ spectrum. The vibrational

spacings are $\sim$145 meV for both progressions: the peaks, however, appear in different excitation energies in the $I(A_1)$ and $I(B_1)$ spectra. The $I(B_1)$ spectrum in Fig. 3(c) is well described by overlapping seven Voigt profiles whose Gaussian and Lorentzian widths are 30 and 170 meV, respectively. The $I(A_1)$ spectrum in Fig. 3 (a), on the other hand, is well described by one broad component, whose Gaussian and Lorentzian widths are 30 and 440 meV, respectively, and five narrow lines whose Gaussian and Lorentzian widths are 30 and 170 meV, respectively.

At first glance, one may consider the observed vibrational progression as the symmetric stretching mode, $(v_1, 0)$, in the A_1 and B_1 states, respectively. Note, however, that one can expect that the A_1 state is bent and thus the bending vibration is highly excited. The frequency of the bending vibration is $\sim$100 meV [12,15] or even lower in the Franck-Condon region where the excitation takes place. Thus the vibrational spacing is comparable with the natural lifetime width $\Gamma \sim 80$ meV of the core-hole state [21]. In addition, each vibrational component is expected to have inhomogeneous broadening of $\sim$20 meV, owing to the different rotational components in the ground state of the sample gas at room temperature. These may explain that the vibrational structure is not resolved on the lower-energy side of the $I(A_1)$ spectrum. If this is the case, however, one cannot expect to see the vibrational structure on the higher-energy side either. Note also that the Lorentzian width of 170 meV obtained by the fitting is significantly larger than expected.

In order to answer the questions given above, we have simulated the excitation spectra by using reliable *ab initio* potential energy surfaces (PES) of the core-excited state. Since the details of the calculations will be discussed elsewhere, we briefly describe the present numerical calculations. In all the calculations reported in this article, the symmetry group of the molecule is assumed to be always C_{2v}. Symmetric stretching and bending modes are taken into account, but asymmetric stretching is neglected. The *ab initio* PES of the C $1s^{-1}2\pi_u$ core-excited state is calculated at the level of multiconfiguration self-consistent-field theory [22] with the active space constructed from $3a_1$-$7a_1$, $1b_1$-$2b_1$, $1a_2$, $2b_2$-$5b_2$ orbitals. The calculations of the core-hole state are achieved by keeping the C $1s$ core orbital ($2a_1$) singly occupied, but the degree of electron spin is fully taken into account. After the above calculations, we optimize the C $1s$ core orbital to estimate the effect of the orbital relaxation: this relaxation causes almost constant energy shift of the PES. The aug-cc-pVTZ basis set of Dunning [23] is used. All the calculations are performed by using the MOLPRO package [24].

Figure 3(d) shows the theoretical $I(B_1)$ spectrum together with each vibrational component: each component is described by a Lorentzian profile with the width of 180 meV. This value was chosen because it gives the best agreement with the experimental spectrum. Not only the global feature but also the detailed vibrational structures are in good agreement with the experimental spectrum.

FIG. 3. Symmetry-resolved excitation spectra. (a),(c) Experimental excitation spectra $I(A_1)$ and $I(B_1)$, respectively. Thick solid lines: the results of the fitting with some Voigt profiles given by the thin solid lines. (b),(d) Theoretical excitation spectra $I(A_1)$ and $I(B_1)$, respectively. Thick solid lines: the spectra calculated in the adiababic representation. Thin solid lines in (d): contributions from each vibrational component. Dashed lines: the spectra calculated taking into account the nonadiabatic effect using a simple approximation. See text for details.

Thus, the theoretical calculation confirms that the observed progression is indeed the progression $(\nu_1, 0)$ of the symmetric stretching mode. The branching ratio to each vibrational component is very sensitive to the stable geometry of the core-excited state. The present theoretical investigation indicates that the bond length in stable geometry of the core-excited B_1 state is 1.22 Å, i.e., 0.06 Å longer than that of the ground state, in excellent agreement with the value empirically obtained by Kukk $et\ al.$ [15].

The calculated $I(A_1)$ spectrum is presented in Fig. 3(b). Each vibrational component (not shown in the figure) is described by the Lorentzian profile with the width 180 meV as in Fig. 3(d). The theoretical calculation reproduces the global broad feature well but does not reproduce the vibrational structure because of the dense vibrational components of the highly excited bending mode, as expected. Changing the Lorentzian width to ~100 meV does not change the result significantly.

In order to explain the vibrational structure observed in the $I(A_1)$ spectrum and the unexpected large Lorentzian widths in both $I(A_1)$ and $I(B_1)$ spectra, one should take into account the nonadiabatic coupling between the A_1 and B_1 states neglected in the present theoretical calculation. This nonadiabatic effect, often referred to as the dynamical Renner-Teller effect [13], is caused by the coupling between the bending nuclear motion and the electronic motion. Then, the vibronic eigenstates are, in principle, obtained by solving the Schrödinger equation including the nonadiabatic coupling term. Here, we take into account the contributions of the nonadiabatic coupling only qualitatively by using a very simple approximation. We assume that the vibronic states are roughly represented in terms of a combination of the A_1 and B_1 adiabatic eigenstates. Then, the excitation spectrum may be approximated by a weighted sum of the $I(A_1)$ and $I(B_1)$ spectra calculated in the adiabatic representation with a little energy shift: this energy shift, in principle, represents the magnitude of the coupling. In Fig. 3(b), we show the $I(A_1)$ spectrum (dashed line) calculated as the sum of the adiabatic $I(A_1)$ and $I(B_1)$ spectra weighted with the ratio of $A_1 : B_1 \sim 1 : 0.2$. The calculation, taking into account the vibronic coupling in this way, reproduces the experimental $I(A_1)$ spectrum well and illustrates that the vibrational structure in the $I(A_1)$ spectrum originates from the symmetric stretching mode in the B_1 state. In Fig. 3(d), we show the $I(B_1)$ spectrum (dashed line) calculated in a similar way. The calculation well reproduces the observed spectrum. The Lorentzian widths adopted in these calculations are not 180 meV but 110 meV, illustrating that the apparent broadening of the Lorentzian component in the experimental spectra is mostly due to the overlap of the broad component originating from the adiabatic $I(A_1)$ spectrum.

In conclusion, we have measured symmetry-resolved excitation spectra for the C $1s \rightarrow 2\pi_u$ A_1 and B_1 resonances for the first time. $Ab\ initio$ calculations for the adiabatic excitation spectra $I(A_1)$ and $I(B_1)$ explain only partially the observed vibrational properties. The weighted sum of the adiabatic $I(A_1)$ and $I(B_1)$ spectra gives reasonable agreement with the experimental results, illustrating the essential role of the nonadiabatic coupling between A_1 and B_1. $Ab\ initio$ calculations including the nonadiabatic coupling are under consideration.

---

*Corresponding author.
Electronic address: ueda@tagen.tohoku.ac.jp.
[1] C. T. Chen, Y. Ma, and F. Sette, Phys. Rev. A **40**, 6737 (1989).
[2] F. X. Gadea $et\ al.$, Phys. Rev. Lett. **66**, 883 (1991).
[3] G. Remmers, M. Domke, and G. Kaindl, Phys. Rev. A **47**, 3085 (1993).
[4] N. Saito and I. H. Suzuki, Phys. Rev. Lett. **61**, 2740 (1988).
[5] A. Yagishita $et\ al.$, Phys. Rev. Lett. **62**, 36 (1989).
[6] K. Lee $et\ al.$, J. Chem. Phys. **93**, 7936 (1990).
[7] E. Shigemasa $et\ al.$, Phys. Rev. A **45**, 2915 (1992).
[8] R. N. Zare, Mol. Photochem. **4**, 1 (1972).
[9] G. E. Busch and K. R. Wilson, J. Chem. Phys. **56**, 3638 (1972).
[10] A. Yagishita, E. Shigemasa, and N. Kosugi, Phys. Rev. Lett. **72**, 3961 (1994).
[11] N. Kosugi, J. Electron Spectrosc. Relat. Phenom. **79**, 351 (1996).
[12] J. Adachi $et\ al.$, J. Chem. Phys. **107**, 4919 (1997).
[13] G. Herzberg, $Infrared\ and\ Raman\ Spectra\ of\ Polyatomic\ Molecules$ (Van Nostrand, New York, 1973).
[14] G. R. Wight and C. E. Brion, J. Electron Spectrosc. Relat. Phenom. **3**, 191 (1973).
[15] E. Kukk, J. D. Bozek, and N. Berrah, Phys. Rev. A **62**, 032708 (2000).
[16] Y. Muramatsu $et\ al.$ (to be published).
[17] H. Ohashi $et\ al.$, Nucl. Instrum. Methods Phys. Res., Sect. A **467−468**, 533 (2001).
[18] T. Tanaka and H. Kitamura, Nucl. Instrum. Methods Phys. Res., Sect. A **364**, 368 (1995); J. Synchrotron Radiat. **3**, 47 (1996).
[19] K. Ueda $et\ al.$, Nucl. Instrum. Methods Phys. Res., Sect. A **467−468**, 1502 (2001).
[20] K. C. Prince $et\ al.$, J. Phys. B **32**, 2551 (1999).
[21] A. Kivimäki $et\ al.$, Phys. Rev. Lett. **79**, 998 (1997).
[22] H.-J. Werner and P. J. Knowles, J. Chem. Phys. **82**, 5053 (1985).
[23] T. H. Dunning, Jr., J. Chem. Phys. **90**, 1007 (1989).
[24] MOLPRO is a package of $ab\ initio$ programs written by H.-J. Werner and P. J. Knowles, with contributions from R. D. Amos $et\ al.$